

NOTES AND CORRESPONDENCE

Persistence of Wintertime 500 mb Height Anomalies over the Central Pacific

JOHN D. HOREL

Climate Research Group, Scripps Institution of Oceanography, La Jolla, CA 92093

17 October 1984 and 6 June 1985

ABSTRACT

The persistence of daily 500 mb geopotential height anomalies during the 17 winters from 1966 to 1982 is documented for a region over the central Pacific that is noted for its frequent blocking activity. Persistence is expressed here in terms of the degree to which a height value remains constant during the next several days. For a 9 grid-point region centered on 50°N, 165°W, blocks (large positive geopotential height anomalies) tend to be less persistent than negative height anomalies between -100 and -200 m. The greater persistence of negative height anomalies in this region is related to periods of stronger than normal zonal flow centered near 40°N (high zonal index). These periods of stronger than normal zonal flow are more persistent than expected of a first-order autoregressive process.

1. Introduction

This note addresses a question which may seem to have been answered many times before: are blocks in the high latitudes over the central Pacific the most persistent regional circulation feature in that area? Persistence is expressed here in terms of the degree to which a geopotential height value at a grid point remains unchanged during the following days. For example, a block over the central Pacific (large geopotential height value at 50°N) is persistent if its amplitude does not change by more than a certain amount during the next several days.

The difficulty in answering this question based on the results of previous investigators of blocking (e.g. Hartmann and Ghan, 1980; Charney *et al.*, 1981; Dole and Gordon, 1983; Shukla and Mo, 1983; Knox and Hay, 1984) arises from their definition of persistence. These investigators define persistence in terms of periods during which geopotential height (at a point, along a latitude circle, within a region, etc.) exceeds a specified threshold for a specified duration. Since the heights in excess of the threshold may vary considerably from day-to-day as the block amplifies, shifts in position, and eventually decays, such episodes may not be persistent as defined here.

Interest in the persistence of high amplitude blocking patterns relative to the persistence of other regional flow configurations is motivated by recent numerical work by Roads (1985) with a two-level nonlinear quasi-geostrophic model. Roads found that the most persistent state was characterized by strong zonal flow in the center of the channel; high amplitude blocking features in his model were more transient. These persistent zonal flows are associated with skewed distributions of height values to the north and south of the maximum

zonal flow, i.e. low height values are more frequent at high latitudes (positive skewness) while large height values are more frequent at low latitudes (negative skewness). These numerical results agree with the observed skewness of geopotential height values in the central Pacific (White, 1980; Dole and Gordon, 1983). For selected parameter ranges in a nonlinear equivalent barotropic model on a sphere, Legras and Ghil (1985) also found the persistence of zonal flow conditions to be greater than that of blocking flows.

The purpose of this note is to document the persistence of geopotential height anomalies over the central Pacific as a function of their sign and their magnitude. It will be shown that stronger than normal zonal flows are more persistent than blocks in this area. The intent here is not to perform another exhaustive study on blocking but instead to focus on a limited region where previous studies have indicated that blocking is prevalent.

2. Data

National Meteorological Center twice-daily analyses of 500 mb geopotential height are used. The period of investigation consists of 17 winter seasons from 1965/66 to 1981/82. Initially, 120-day winter seasons, starting November 15 and ending (except leap years) March 14, are used.

Nine grid points in each of two regions were selected as shown in Fig. 1. Region A, centered on 50°N, 165°W, corresponds to the area of maximum blocking activity as defined by Dole and Gordon (1983). Multiple grid points in each region are used so as to minimize the effects of occasional errors in the time series at individual grid points. The difference between the averages of geopotential height in Regions A and B will

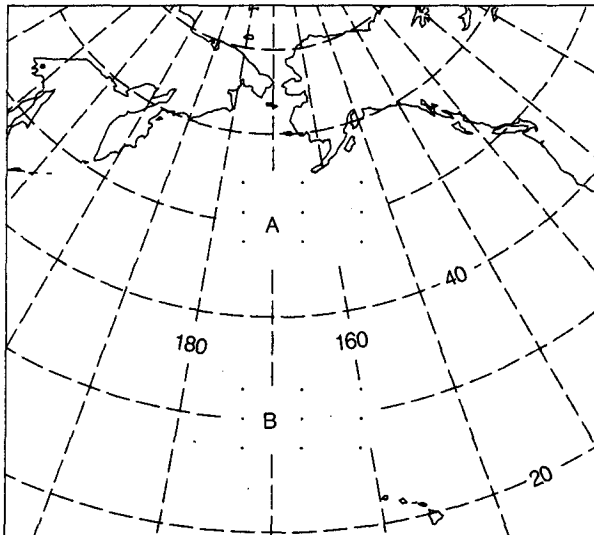


FIG. 1. Locations of the 18 grid points used in this study. The grid points centered near 50°N, 165°W are located in the area of maximum blocking activity as defined by Dole and Gordon (1983).

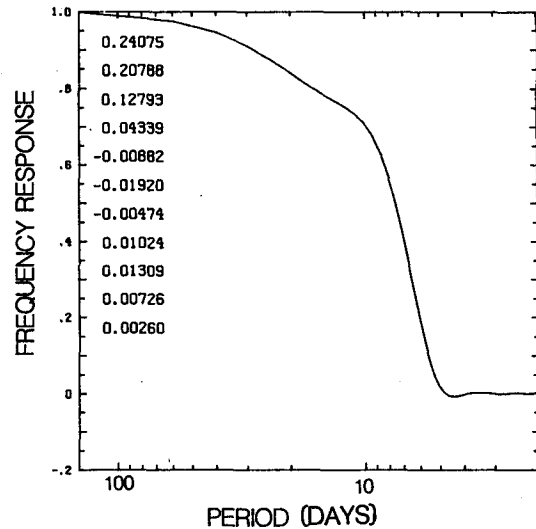


FIG. 2. Frequency response of the 21-day running mean filter with the weights listed along the left edge of the figure (the top number is for time t ; the second number is for times $t + 1$, etc.).

be used as an indicator of the strength of the zonal flow near 40°N, 165°W.

The twice-daily analyses were averaged together to obtain daily means. Climatological means at each grid point and for each day of the season were computed from the 17 years of observations. Since climatological daily means derived from only 17 years of data may be influenced by occasional errors in the data, the means were smoothed by using three passes of a five-day running mean smoother. The smoothed climatological means were subtracted from the original observations and the resulting departures are referred to as the unfiltered data.

In addition, fluctuations with periods less than five days were eliminated from the data by applying a 21-point running mean smoother to the data. The response function and weights of this smoother are shown in Fig. 2. The first and last 10 days of each winter season, which could not be smoothed by the 21-point filter, were then dropped, leaving 100 days during each season for both unfiltered and filtered datasets.

3. Results

The unfiltered daily height anomalies at each of the 9 grid points in Region A (see Fig. 1), were collected into 8 bins: the first bin contains all of the height anomalies that were less than -300 m, bins 2-7 cover successive 100 m intervals (e.g. bin 2 contains all the height values between -300 and -200 m) while the last bin contains all the values greater than 300 m. The number of elements in each bin is shown in Fig. 3 (heavy solid line). The positively skewed distribution of geopotential height in this region is evident with

more values greater than 300 m than less than -300 m.

The persistence of the height anomalies as a function of their amplitude and their sign was determined. The height value at a particular grid point on day t was

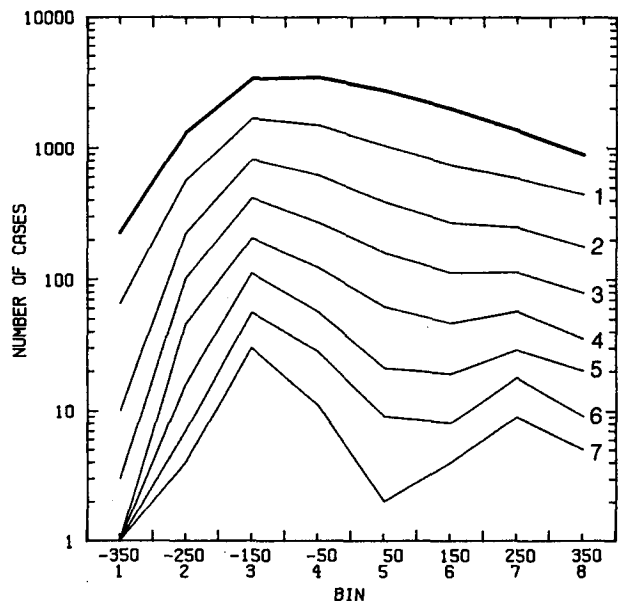


FIG. 3. The number of cases of geopotential height anomalies in Region A which fall within the following bins (heavy line): bin 1 includes all values less than -300 m; bins 2-7 cover 100 m intervals starting with the interval -300 to -200 m; bin 8 includes all values greater than 300 m. The central value of each bin is shown at the bottom. The other curves represent the number of cases of height values in each bin that changed by less than ± 50 m during the following 1-7 days. See Section 3 for further details.

compared to the height values at that grid point on the following 25 days. The number of cases where the height value on day t changed by less than the bin width (± 50 m) during the following 1–7 days are shown in Fig. 3. All initial height anomalies are treated the same whether they lie in the center of a bin or near an edge; for example, if an initial height anomaly of 199 m remains within the range 199 ± 50 m for three additional days, then one unit is added to the sixth bin for durations 1–3 days.

Although the number of initial height anomalies in bins 3 (-200 to -100 m) and 4 (-100 to 0 m) is nearly the same, Fig. 3 indicates that the height anomalies in bin 3 are more persistent than any other comparable range of height anomalies. For example, over 400 cases of initial height values between -200 and -100 m changed by less than ± 50 m during the next 3 days while only 120 such cases occurred for initial values between 100 and 200 m. There is a slight tendency for large positive anomalies (between 200 and 300 m) to be more persistent than other positive anomalies, however the number of such cases is small.

Several points need to be made regarding the analysis approach used here. The number of cases in each bin and duration are sensitive to both the bin width and the allowable change criterion (± 50 m). Experimentation with different values of these parameters indicated that the persistence of the height anomalies between -200 and -100 m remained higher than that of any other range of height anomalies. A more serious concern is that many of the cases in Fig. 3 are not independent of one another; the 9 grid points generally have similar values on each day. Also, if the height value starting on day t persists for 7 days, then the value on day $t + 1$ will persist probably for at least 6 days, that on day $t + 2$ for at least 5 days, etc. Thus, the number of cases shown in Fig. 3 is an overestimate of the number of independent cases. This point will be discussed further.

The unfiltered data set used in Fig. 3 contains short period, synoptic-scale fluctuations that may mask or otherwise distort persistent atmospheric states. As described in Section 2, another dataset was created such that fluctuations with periods less than five days were removed. The results from the filtered data are shown in Fig. 4. Not surprisingly, the filtered height values in all bins remain within the limits ± 50 m for longer durations. The tendency for height anomalies between -200 and -100 m to be more persistent than any other height anomalies is even more pronounced; over 100 cases lasted for 15 days; four cases lasted 25 days (not shown).

The persistence of height anomalies in Region B was also determined but will not be shown here. As described by White (1980), the height anomalies in Region B are negatively skewed (positive anomalies are more frequent). Roughly 900 cases of filtered height anomalies between 0 and 100 m remained within the

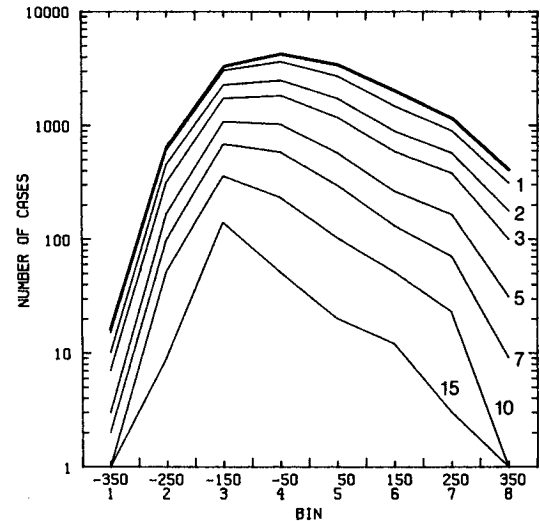


FIG. 4. As in Fig. 3 except for the filtered data set (fluctuations with periods less than 5 days removed). Curves for durations of 1, 2, 3, 5, 7, 10, and 15 days are shown.

limit ± 25 m for 10 days while less than 200 cases between 0 and -100 m remained within that limit for the same duration. (The allowable change was reduced to ± 25 m because the variability of geopotential height in Region B is less.)

A crude index of the zonal flow in the north central Pacific was computed by subtracting the daily average of the nine height values in Region A from a similar average for Region B. The difference in height was then converted to a zonal wind value using the geostrophic approximation, i.e., a difference of 50 m is equivalent to roughly 2.5 m s^{-1} . From the 1930s to the 1950s, such zonal flow indices were commonly used as a diagnostic of the regional and hemispheric circulation (e.g., Namias, 1950).

The time series of the filtered zonal wind index is shown in Fig. 5. Periods of weaker than normal zonal flow, such as December 1965, tend to grow in amplitude and decay faster than periods of stronger than normal zonal flow, such as February 1970.

Figure 6 summarizes the persistence of the regional zonal wind index. As expected from the previous results, zonal wind anomalies between 5 and 10 m s^{-1} above normal are more persistent than any other comparable range of anomalies. Roughly 80 cases in bin 3 remained within the limit $\pm 2.5 \text{ m s}^{-1}$ for at least 10 days. There is also a slight tendency for anomalies between -5 and -10 m s^{-1} to be more persistent for long durations than other negative anomalies.

In order to verify that the results in Fig. 6 were not biased by the greater variability of geopotential height in Region A, an index derived from the difference between the standardized anomalies in Regions A and B was also derived. The persistence of the standardized index was nearly the same as that shown in Fig. 6.

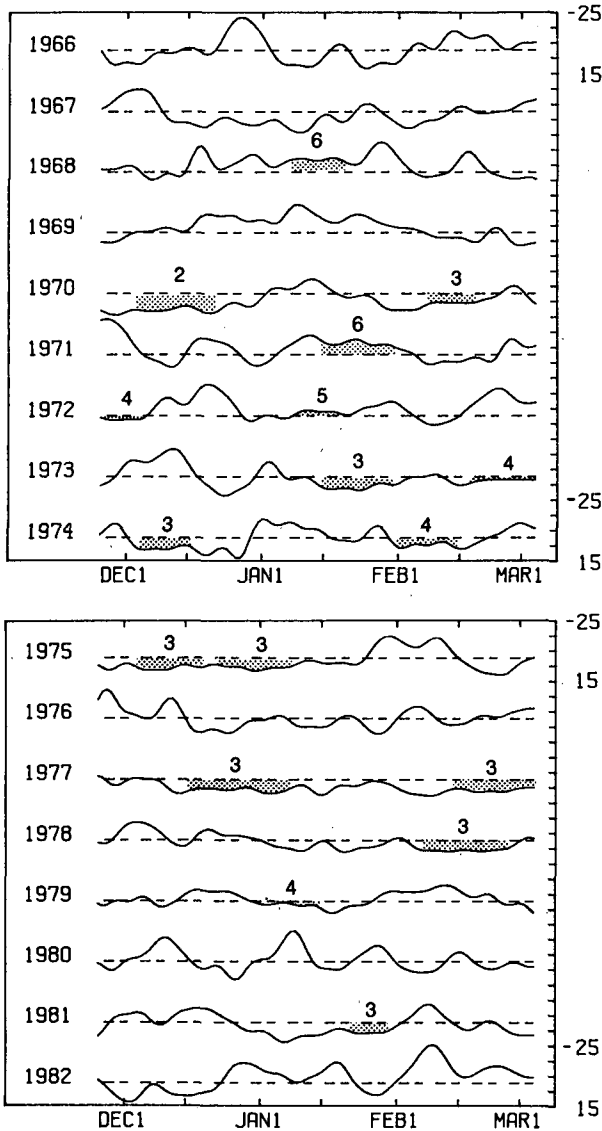


FIG. 5. Time series of the filtered zonal wind index described in Section 3 (in $m s^{-1}$). The time series is inverted so that blocking episodes (periods with weaker than normal zonal flow) are above the zero line. Periods during which initial index values remained within the limit $\pm 2.5 m s^{-1}$ for at least 10 days are indicated by stippling. The numbers above the stippled areas denote the bin number of the initial index value.

Although 80 cases in bin 3 persisted for 10 or more days, these cases resulted from only 9 independent events. Independent events were identified subjectively from overlapping regimes by choosing the event which had the longest duration. The dates of the independent events in all of the bins are delineated in Fig. 5. Note that only three weaker than normal zonal flow cases were observed to last longer than 10 days (January 1968, January 1971, and January 1972). On the other hand, 14 events of stronger than normal flow were ob-

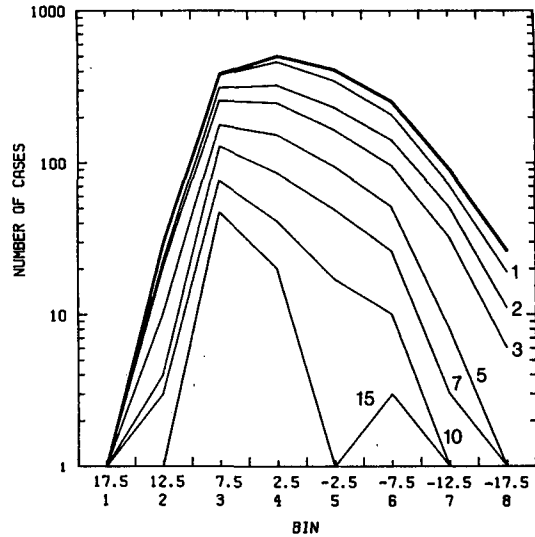


FIG. 6. As in Fig. 3 except for the filtered zonal wind index. The allowable change criterion is $\pm 2.5 m s^{-1}$. The center value of each bin is indicated at the bottom (in $m s^{-1}$).

served to last longer than 10 days. Hereafter, the 10 events in bins 2 and 3 are considered to represent a high zonal index state. It should be remembered that the number of cases in each bin (and the total number of independent events) is a function of the bin width and allowable change criterion; the ratio between the number of persistent blocks to persistent high zonal index states for a given choice of parameter values is the important result.

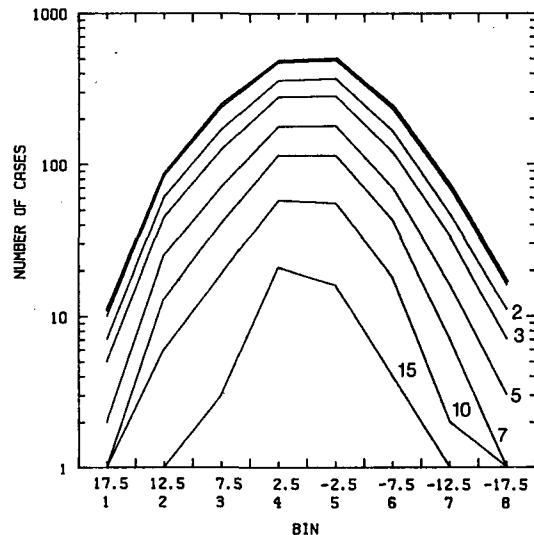


FIG. 7. As in Fig. 6 except for the 170-year red-noise data set. The total number of cases in each bin was divided by 10 in order to be comparable to the 17-year dataset. The number of cases that lasted an additional day are nearly identical to the initial distribution (heavy curve). See Section 4 for further details.

4. Comparison to red-noise processes

Gutzler and Mo (1983) computed autocorrelation statistics of the 500 mb height field and found that the memory of the atmospheric circulation tends to fall off faster than that expected of a first-order autoregressive (red noise) process. Trenberth (1984) has shown that Gutzler and Mo underestimated the amount of autocorrelation in the 500 mb height field because they eliminated interannual variability from their data.

The autocorrelations for selected lags of the unfiltered zonal wind index were computed using the procedure recommended by Trenberth. The autocorrelations for lags of 1, 2, 5, and 10 days are 0.89, 0.74, 0.50, and 0.13, respectively. For a first-order autoregressive process, the autocorrelation at lag τ is $r_\tau(\tau) = r(1)^\tau$, where $r(1)$ is the 1-day lag autocorrelation. Using this relationship, the red-noise autocorrelations for lags of 2, 5, and 10 days of the zonal wind index were found to be 0.79, 0.56, and 0.31 respectively. Thus, even though the analysis procedure of Gutzler and Mo underestimated the actual autocorrelation, their principal result appears to be correct: the observed autocorrelations of 500 mb circulation anomalies fall off more rapidly than a red-noise process would suggest.

One possible reason for the rapid decay of the autocorrelation of the zonal wind index over the north central Pacific is that autocorrelation statistics are based on the entire range of index values; the greater persistence of stronger than normal zonal flow conditions shown in the previous section may be masked by the lesser persistence of weaker than normal zonal flows. In order to determine whether the persistence of the high zonal index state is attributable only to red-noise processes, a 170-year data set was created using the mean (\bar{X}), standard deviation (σ), and 1-day lag autocorrelation of the unfiltered zonal index [$r(1) = 0.89$] according to the following:

$$X(t+1) = \bar{X} + r(1)[X(t) - \bar{X}] + [1 - r^2(1)]^{1/2} \sigma \epsilon(t)$$

where $\epsilon(t)$ is a number drawn at random from a normally distributed population with a standard deviation equal to 1.0. This red-noise dataset was then subjected to the same filtering and analysis as the data used before. Note that it is assumed here that the skewness of the distribution of the zonal index values arises from other than red-noise processes.

Figure 7 summarizes the initial values of the index which changed by less than $\pm 2.5 \text{ m s}^{-1}$ during the next 1–15 days based on the 170-year red-noise dataset. Since the initial distribution of the index values is nearly Gaussian, the most persistent values lie between -5 and 5 m s^{-1} . The observed number of cases that persist for long durations in Fig. 6 differs from the distribution derived from a red-noise process in two important respects. First, the observed index values between 0 and

5 m s^{-1} decay more rapidly than a red-noise process would suggest. Second, the high zonal index state persists much more frequently than expected from a red-noise process, e.g., 80 cases (9 independent events) between -5 and -10 m s^{-1} lasted 10 days while only 15 cases in this category lasted 10 days (2 independent events) in Fig. 7. Even considering the fewer number of initial cases in bin 3 in Fig. 7, the persistence of the high zonal index state in Fig. 6 stands out above that expected of a red-noise process.

Finally, it should be noted that the persistence of the zonal index is not simply a reflection of the positive skewness of their frequency distribution. In other words, even though strong zonal flow conditions occur more often over the north central Pacific than weak zonal flows, there is no reason to expect *a priori* that strong zonal flows will be persistent. In order to verify this point, another 170-year dataset was constructed by randomly picking values from the skewed initial frequency distribution shown in Fig. 6. The persistence of this skewed, random population was then determined as for Figs. 6 and 7 (not shown). While more initial values in bins 3 and 4 remained within the limits of $\pm 2.5 \text{ m s}^{-1}$ during the following day, no values in any bins remained within those limits for more than 2 days. Hence, the results of this section indicate that the persistence of strong zonal flow states appears to be greater than that expected of random or red-noise populations.

5. Discussion

The purpose of this note has been to look at the persistence of regional circulation anomalies over the North Pacific from a different perspective than previous investigators. Analyses of blocking emphasize the infrequent occurrences of extreme height values whereas this study has been concerned with the persistence of height anomalies over the entire range of initial anomaly amplitudes. Even though the extremes of the frequency distribution of height anomalies may represent spectacular and easily recognizable features on weather maps, the results of this study indicate that they are not very persistent in comparison to less obvious (and more frequent) periods of moderately intense zonal flow across the north central Pacific.

Dole and Gordon (1983) documented the initial 12-hour tendency of height anomalies as a function of anomaly amplitude. Although they emphasized comparisons of large positive and negative height anomalies in the central Pacific, many of their results corroborate those described in Section 3. For example, they found that small negative anomalies tended to change less during the next 12 hours than positive anomalies (see their Fig. 11a).

The central Pacific region has been treated in this paper as if it were distinct from the rest of the planetary-

scale circulation. Obviously, the stronger than normal zonal flow state near 40°N, 165°W is part of larger scale circulation changes. Horel (1985) identified low wavenumber quasi-stationary regimes from the Northern Hemisphere 500 mb height field. The dominant regime was a superposition of a wavenumber 3 pattern upon a large zonally symmetric component, resulting in strong zonal flows across the central Pacific. Of the 10 high zonal index states identified here, 8 of them overlapped with hemispheric quasi-stationary regimes listed by Horel (1985).

It has been expected for many years based on theoretical studies of wave-mean flow interaction (e.g. Charney and Devore, 1979) that distinct periods exist when the atmospheric circulation locks into preferred states and that these states would be more predictable by medium-range numerical forecasts than other more transient periods. Most of the attention has been focussed on the prediction of high amplitude blocks. The results of Section 3 suggest that if the variable amplitude of blocks over the central Pacific is considered, then blocks can hardly be called persistent. The general inability of numerical models to forecast blocks successfully may reflect the fact that their rapid growth and decay are difficult to simulate. More success in medium range forecasting may be possible if attention is placed on periods of stronger than normal zonal flows and their relationship to the planetary scale circulation.

Acknowledgments. This research was supported by the Climate Dynamics Program of the National Science Foundation under Grant ATM-8300747. I would like to thank J. Roads, Climate Research Group for initially suggesting the definition of persistence used here and for many helpful discussions. I also appreciate the use-

ful comments and suggestions of R. Dole, Massachusetts Institute of Technology, H. van den Dool, University of Maryland, and M. Ghil, Courant Institute of Mathematical Sciences.

REFERENCES

- Charney, J. G., and J. G. Devore, 1979: Multiple flow equilibria in the atmosphere and blocking. *J. Atmos. Sci.*, **36**, 1205-1216.
- , J. Shukla and K. C. Mo, 1981: Comparison of a barotropic blocking theory with observations. *J. Atmos. Sci.*, **38**, 762-779.
- Dole, R. M., and N. D. Gordon, 1983: Persistent anomalies of the extratropical Northern Hemisphere wintertime circulation: Geographical distribution and regional persistence characteristics. *Mon. Wea. Rev.*, **111**, 1567-1586.
- Gutzler, D. S., and K. C. Mo, 1983: Autocorrelation of Northern Hemisphere geopotential heights. *Mon. Wea. Rev.*, **111**, 155-164.
- Hartmann, D. L., and S. J. Ghan, 1980: A statistical study of the dynamics of blocking. *Mon. Wea. Rev.*, **108**, 1144-1159.
- Horel, J. D., 1985: The persistence of the 500 mb height field during Northern Hemisphere winter. *Mon. Wea. Rev.*, **113**, 2030-2042.
- Knox, J. L., and J. E. Hay, 1984: Blocking signatures in the Northern Hemisphere: rationale and identification. *Atmos. Ocean*, **22**, 36-47.
- Legras, B., and M. Ghil, 1985: Persistent anomalies, blocking and variations in atmospheric predictability. *J. Atmos. Sci.*, **42**, 433-471.
- Namias, J., 1950: The index cycle and its role in the general circulation. *J. Meteor.*, **7**, 130-139.
- Roads, J. O., 1985: Temporal variations in predictability. *J. Atmos. Sci.*, **42**, 884-903.
- Shukla, J., and K. C. Mo, 1983: Seasonal and geographical variation of blocking. *Mon. Wea. Rev.*, **111**, 388-402.
- Trenberth, K. E., 1984: Some effects of finite sample size and persistence on meteorological statistics. Part I: Autocorrelations. *Mon. Wea. Rev.*, **112**, 2359-2368.
- White, G. H., 1980: Skewness, kurtosis, and extreme values of Northern Hemisphere geopotential heights. *Mon. Wea. Rev.*, **108**, 1446-1455.